Since January 2020 Elsevier has created a COVID-19 resource centre with free information in English and Mandarin on the novel coronavirus COVID-19. The COVID-19 resource centre is hosted on Elsevier Connect, the company's public news and information website.

Results in Physics 38 (2022) 105652

Contents lists available at ScienceDirect

Results in Physics

journal homepage: www.elsevier.com/locate/rinp

Assessing the potential impact of COVID-19 Omicron variant: Insight through a fractional piecewise model

Xiao-Ping Li [a,1], Mahmoud H. DarAssi [b,1], Muhammad Altaf Khan [c,1], C.W. Chukwu [d,1], Mohammad Y. Alshahrani [e,1], Mesfer Al Shahrani [e,1], Muhammad Bilal Riaz [f,g,c,*,1]

[a] School of Mathematics and Information Science, Xiangnan University, Chenzhou, 423000, Hunan, PR China
[b] Department of Basic Sciences, Princess Sumaya University for Technology, Amman 11941, Jordan
[c] Institute for Ground Water Studies, Faculty of Natural and Agricultural Sciences, University of the Free State, South Africa
[d] Division of Infectious Diseases and Global Public Health, University of California, San Diego, CA, USA
[e] Department of Clinical Laboratory Sciences, College of Applied Medical Sciences, King Khalid University, P.O. Box 61413, Abha, 9088, Saudi Arabia
[f] Department of Automation, Biomechanics and Mechatronics, Lodz University of Technology, 1/15 Stefanowskiego St., 90-924 Lodz, Poland
[g] Department of Mathematics, University of Management and Technology, 54770, Lahore, Pakistan

ARTICLE INFO

Keywords:
Omicron
COVID-19
Numerical simulation
Fractional model
Piecewise model

ABSTRACT

We consider a new mathematical model for the COVID-19 disease with Omicron variant mutation. We formulate in details the modeling of the problem with omicron variant in classical differential equations. We use the definition of the Atangana–Baleanu derivative and obtain the extended fractional version of the omicron model. We study mathematical results for the fractional model and show the local asymptotical stability of the model for infection-free case if $\mathcal{R}_0 < 1$. We show the global asymptotically stable of the model for the disease free case when $\mathcal{R}_0 \leq 1$. We show the existence and uniqueness of solution of the fractional model. We further extend the fractional order model into piecewise differential equation system and give a numerical algorithm for their numerical simulation. We consider the real cases of COVID-19 in South Africa of the third wave March 2021–Sep 2021 and estimate the model parameters and get $\mathcal{R}_0 \approx 1.4004$. The real parameters values are used to show the graphical results for the fractional and piecewise model.

Introduction

COVID-19 has been a public health concern since its emergence in Wuhan, China, in early December 2019 [1]. The disease has also ravaged most of the world's economy, closure of schools, public facilities, etc. Currently, the uses of vaccination such as Pfizer, AstraZeneca, Moderna, etc., are used to mitigate the spread of the disease to bring this pandemic to an end through immunization against the virus [2]. The world is still facing the COVID-19 infection with their new variants that caused human life in danger. There are so many variants of this infection that have been reported in different parts of the world, such as alpha, beta, etc., among these some were found very dangerous as compared to the original virus. The delta virus is also one of the deadly variants of the COVID-19 which provided a lot of death and infected cases in many countries. The emergence of the new variant known as the Omicron virus of the COVID-19 was reported in South Africa and found very dangerous to human society. The most important features of this virus are its fast spreading among the human population.

The SARS-CoV-2 virus can survive and mutate to different viruses under different survivability or weather conditions, or temperatures [3,4]. Following the advice of WHO's Technical Advisory Group on Virus Evolution, the world health organization (WHO) identified variant B.1.1.529 as a COVID-19 variant of concern on November 26, 2021, and called it Omicron (TAG-VE). This decision was made based on clinical information submitted to the TAG-VE showing Omicron has multiple mutations that may have an impact on its behavior, such as how quickly it spreads and the severity of sickness it produces when compared to other mutations (Delta, Beta variants). Unlike previous COVID-19 variants, Omicron infects persons who have antibodies to earlier SARS-CoV-2 forms, which they acquired through infection or immunization. It is claimed to be highly contagious, with heightened transmissibility and the capacity to evade past infection or vaccination-induced immunity (i.e., immune evasion) [5,6]. This latest mutant of the COVID-19 is known as the Omicron variant has caused more loss

* Corresponding author at: Department of Automation, Biomechanics and Mechatronics, Lodz University of Technology, 1/15 Stefanowskiego St., 90-924 Lodz, Poland.
E-mail address: muhammad.riaz@p.lodz.pl (M.B. Riaz).
[1] All the authors contributed equally to this work.

https://doi.org/10.1016/j.rinp.2022.105652
Received 16 April 2022; Received in revised form 20 May 2022; Accepted 23 May 2022
Available online 30 May 2022

of life to humans and poses a great to even in developed countries such as the US, Canada, Australia, Europe [5,7].

Since the outbreak of coronavirus, several mathematical models are proposed in various ways to control or reduce the risk of disease transmission worldwide. These includes the use integer and fractional modeling frameworks for different countries incorporating non-pharmaceutical interventions/vaccine [8], environmental factors [9,10], dead compartments [11], Omicron variants [8,12–14], social distancing [15], optimal control [16,17], super spreaders [18]. In particular, authors in [15] used an integer order model to quantify the effect of social distancing on the transmission dynamics of the coronavirus spread in South Africa. It suggest that a decrease in the social distancing and relaxation of regulations result in an increase in the number of infected individuals in the community, leading to more infections. Authors in [18,19], used a fractional-order to model the effect of environmental transmission on COVID-19 dynamics for a case study focused on Indonesia and India, respectively. It was found that reduction of environmental transmission parameters will lead to lesser virus transmission in the population. Therefore, to eradicate or control the COVID-19 disease spread, their modeling projects practice proper hygiene, save burial, and other control measures to prevent the spread of the disease. For more details on other models that have used fractional derivatives to model COVID-19, see the following Refs. [11,19–21]. Several other modeling frameworks have been carried out since the emergence of the Omicron variant to look at various ways to understand the disease's transmissibility and controllability in several countries worldwide. An epidemiological study were presented for the case of England between December 2021 and April 2022 [12,22]. Even in areas with high levels of immunity, like as England, the findings imply that Omicron has the potential to cause significant increases in cases, hospital admissions, and fatalities. In addition, other non-pharmaceutical measures may need to be reintroduced to prevent hospital admissions in England from exceeding those seen during the previous peak in winter 2020–2021. Few other fractional models and integer models [8,13,14] that have also modeled Omicron variant incorporating non-pharmaceutical interventions and vaccine [13] while in [8] the authors created and used real data from the United Kingdom to investigate the spread of COVID-19 with and without the Omicron variation and its connection with heart attack.

Fractional calculus has a memory effect, which aids in correctly predicting physical systems or mathematical models. This has led to new advancements in developing new operators such as Riemann–Liouville-Caputo, Atangana–Baleanu ($\mathcal{ABC}$), and Caputo–Fabrizio fractional-order derivatives in integer and non-integer orders that have been proposed to be applied to solve real-world problems, for example, the applications in integrodifferential equations [23], the new advancement and development in fractional operators [24,25], application to epidemiology [26–31], application to wave dynamics equations, [32,33] and other physical problems [34–36] etc. Some recent applications of fractional calculus in physical sciences has been discussed by the authors recently [37–39]. The COVID-19 infection using the Legendre spectral method has been discussed in [37]. The authors in [38] used the fractal–fractional approach to study the Michaelis–Menten Enzymatic Reaction in the fractional derivative. The fractional reaction diffusion problem has been analyzed by the authors in [39]. In the present study, we develop and analyze a mathematical model by applying the Atangana–Baleanu fractional derivative to study the potential impact of the Omicron variant of the COVID-19 virus and suggest possible strategies to reduce its risk of transmission in any community induced by the virus emergent.

The rest of the parts of this manuscript is arranged as follows. Section "Model description" gives the model formulation followed by fractional-order mathematical preliminaries in Section "Preliminaries". While in Section "Mathematical analysis of the model", we present the mathematical analysis of the model in detail. The new concept of the piecewise modeling approach and their related results has been given in Section "Piecewise model". We consider the real data of the South Africa to estimate the model parameters and obtain their graphical results in Section "Numerical simulation". Section "Conclusion" concludes the paper with some discussion on the results.

Model description

The omicron variant which is the new variant of the SARS-CoV-2 originally discovered in South Africa in November 2021. The virus is more dangerous than the original virus of SRAS-CoV-2, so the mathematical modeling and its understanding is very important for the public health authorities. So, we develop a deterministic model for COVID-19 infection which consist of the human population and the SAR-CoV-2 mutant variant Omicron (O) (individuals infected with the new variant known as Omicron infected). The human population is then sub-divided into the susceptible (S), Exposed, (E), Asymptomatic (A), Infectious (I), Omicron infected (O), Hospitalized (H), Dead (D) and the Recovered (R). Therefore, given a total population

$$N(t) = S(t) + E(t) + A(t) + I(t) + O(t) + H(t) + R(t) + D(t).$$

at any time t. Humans are recruited into the population at rate Λ and then becoming susceptible to COVID-19 disease at rate

$$\lambda = \frac{\beta_1 A + \beta_2 I + \beta_3 O + \beta_4 H}{N},$$

after been exposed. β_i for $i = 1, \ldots, 4$ are the disease transmission rates. Here, λ is the force of infection which considers that only individuals in A, I, O or H compartments can transmit the disease. The interaction of the healthy people with the individuals that do not show symptoms (asymptomatic people) become infected and spread the infection further in the population. It is documented that the asymptomatic people have strong immunity and a rare cases of death can be occurred for them, so, we do not add the disease related mortality of the asymptomatic people in our model. The interaction of the healthy people with the individuals that have clear disease symptoms, omicron infected and those hospitalized individuals infect healthy people and spread the infection further, so β_2, β_3 and β_4 measure their disease transmission. The exposed individuals are exposed can then progress to become asymptomatic at the rate $\delta\kappa$ or into the Omicron compartment at rate $\phi\delta$ while the reminder becomes infectious and develops symptoms at the rate $(1 - \kappa - \phi)$. The death rate of the symptomatic, omicron infected and the hospitalized individuals are shown respectively by d_1, d_2 and d_3. ψ_i for $i = 1, \ldots, 4$ respectively show the recovery of the asymptomatic, symptomatic, omicron and hospitalized individuals. The symptomatic and omicron infected people are hospitalized at the rate respectively given by q_1 and q_2. We assume that each class of the model has a natural death rate μ while the recruitment rate of the healthy population is given by Λ. The descriptions of the model classes and their parameters flow are shown in detail in Fig. 1.

A combination of our model assumptions, description, and Fig. 1 yields the following systems of the set of 8 ordinary differential equations:

$$\frac{dS}{dt} = \Lambda - (\mu + \lambda)S, \tag{1}$$

$$\frac{dE}{dt} = \lambda S - (\mu + \delta)E, \tag{2}$$

$$\frac{dA}{dt} = \delta\kappa E - (\mu + \psi_1)A, \tag{3}$$

$$\frac{dI}{dt} = (1 - \kappa - \phi)\delta E - (\mu + \psi_2 + d_1 + q_1)I, \tag{4}$$

$$\frac{dO}{dt} = \phi\delta E - (\mu + \psi_3 + d_2 + q_2)O, \tag{5}$$

$$\frac{dH}{dt} = q_1 I + q_2 O - (\mu + \psi_4 + d_3)H, \tag{6}$$

$$\frac{dR}{dt} = \psi_1 A + \psi_2 I + \psi_3 O + \psi_4 H - \mu R, \tag{7}$$

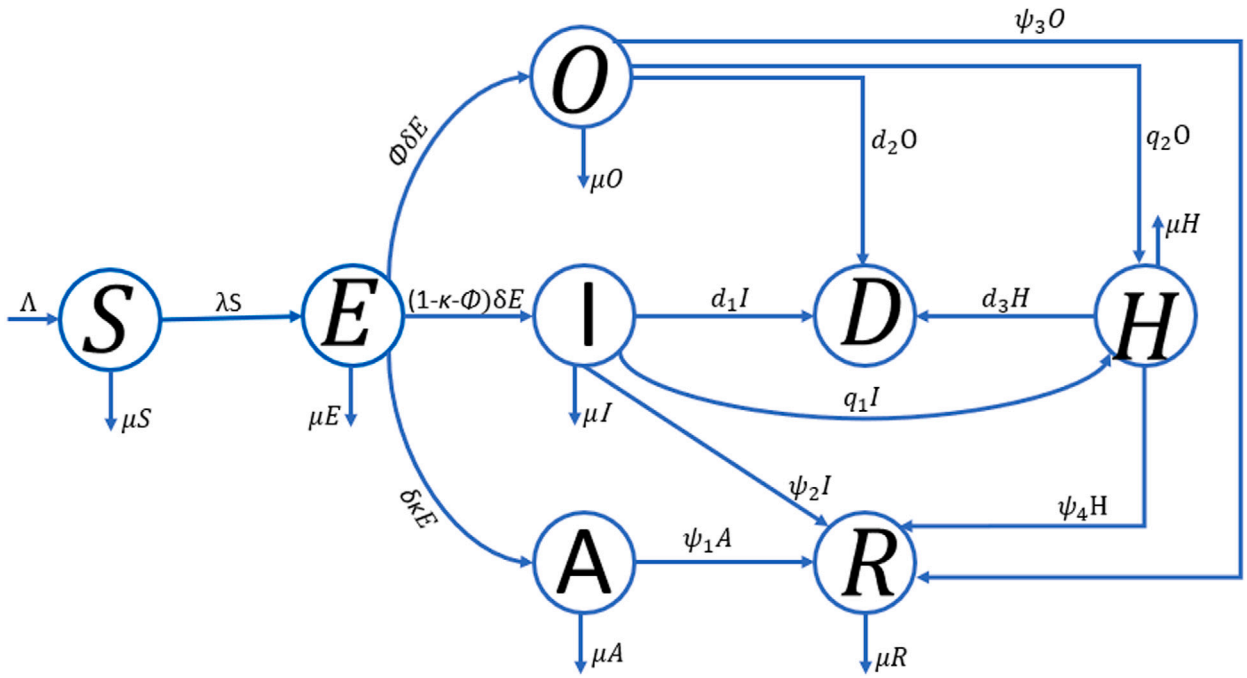

Fig. 1. The diagram describing the transmission dynamics of COVID-19 incorporating the Omicron compartment, (O), in the human population $N(t)$. The solid arrows represent the transitions from distinct compartments to another.

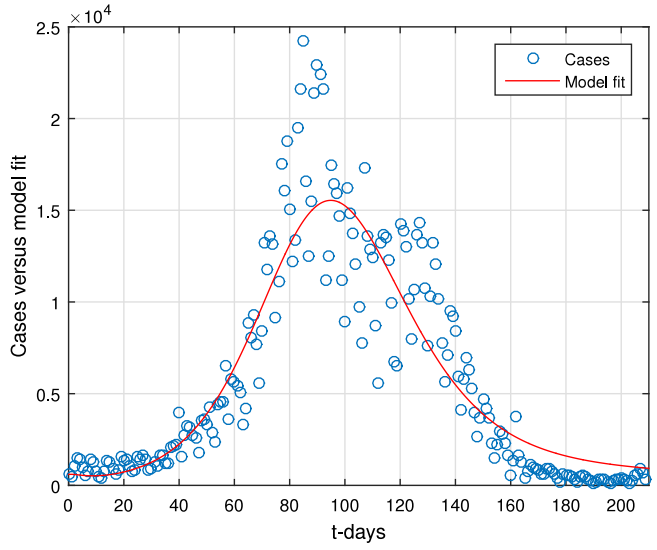

Fig. 2. Data versus model fitting.

Table 1
Details of the model parameters and their numerical value.

Notation	Descriptions	Value	Ref
Λ	Birth rate	2559	Estimated
μ	Natural death rate	$\frac{1}{64.38\times365}$	Estimated
β_1	Contact rate due to A	0.2235	Fitted
β_2	Contact rate to I	0.0763	Fitted
β_3	Contact rate due to O	0.8303	Fitted
β_4	Contact rate due to H	0.3142	Fitted
q_1	Hospitalization rate of symptomatic people	0.0100	Fitted
q_2	Hospitalization rate of omicron infected people	0.5384	Fitted
δ	Incubation period	0.5239	Fitted
κ	Progress to A	0.2599	Fitted
ϕ	Progress to O	0.7356	Fitted
ψ_1	Rate of recovery of asymptomatic	1/(5.1)	[40–42]
ψ_2	Rate of recovery of symptomatic	1/10	[40–42]
ψ_3	Rate of recovery of omicron infected	0.6912	Fitted
ψ_4	Rate of recovery of hospitalized people	1/8	[41]
d_1	Death rate due to infection at I	0.015	[40–42]
d_2	Death rate due to infection ar O	0.0100	Fitted
d_3	Death rate due to infection at H	0.04	[41]

$$\frac{dD}{dt} = d_1 I + d_2 O + d_3 H, \tag{8}$$

subject to the intimal conditions

$$S(0) > 0,\ E(0) \geq 0,\ A(0) \geq 0,\ I(0) \geq 0,\ O(0) \geq 0,$$
$$H(0) \geq 0,\ R(0) \geq 0,\ D(0) \geq 0.$$

We assume that the recovered and the dead compartments do not involve the disease progress. So, in the absence of the equation R and D our model equations (1)–(8) can be reduced to the following system:

$$\begin{cases} \frac{dS}{dt} = \Lambda - (\mu+\lambda)S, \\ \frac{dE}{dt} = \lambda S - Q_0 E, \\ \frac{dA}{dt} = \delta\kappa E - Q_1 A, \\ \frac{dI}{dt} = (1-\kappa-\phi)\delta E - Q_2 I, \\ \frac{dO}{dt} = \phi\delta E - Q_3 O, \\ \frac{dH}{dt} = q_1 I + q_2 O - Q_4 H, \end{cases} \tag{9}$$

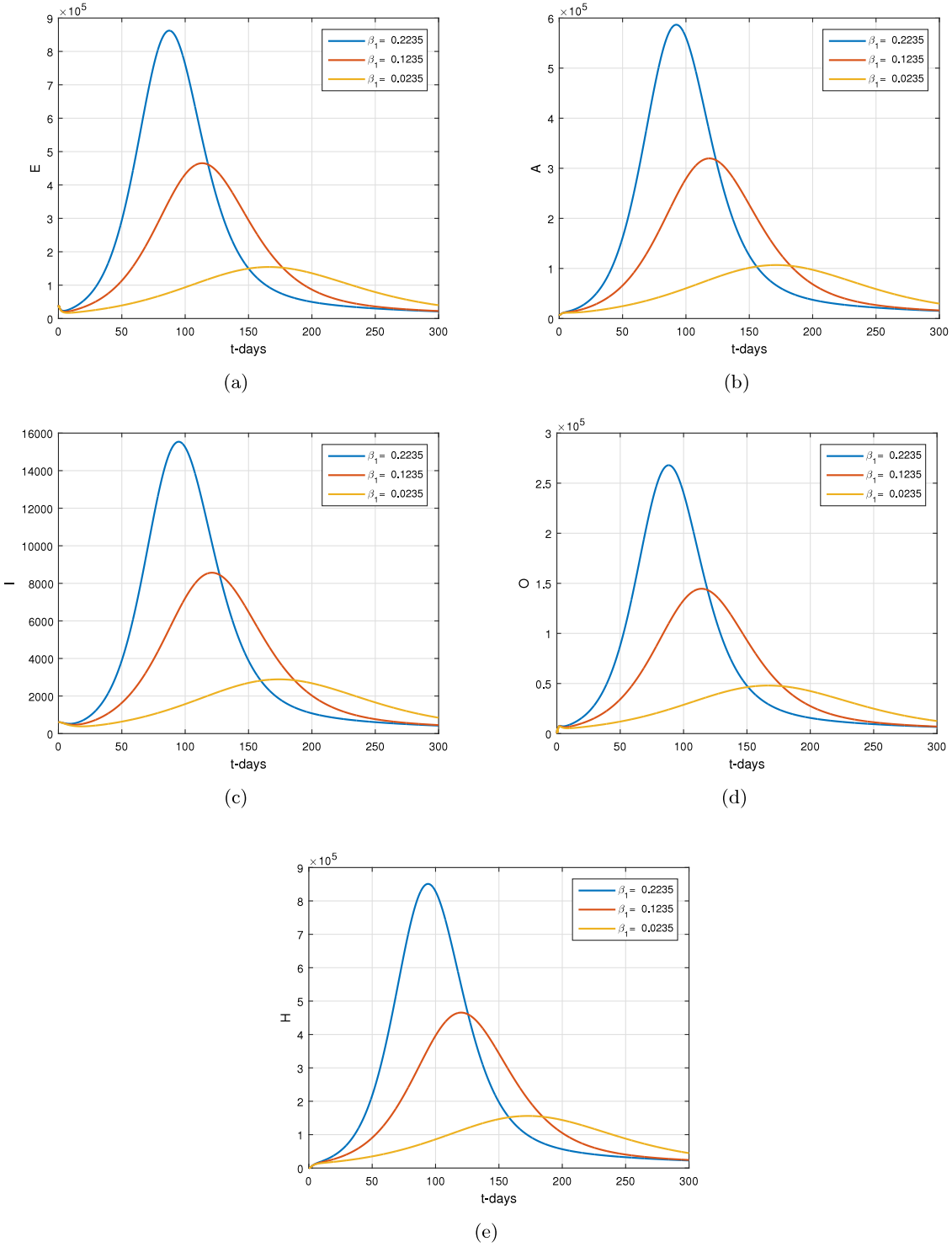

Fig. 3. The effect of β_1 on the infected compartments.

where

$Q_0 = (\mu + \delta),\ Q_1 = (\mu + \psi_1),\ Q_2 = (\mu + \psi_2 + d_1 + q_1),$
$Q_3 = (\mu + \psi_3 + d_2 + q_2)$ and $Q_4 = (\mu + \psi_4 + d_3)$.

Preliminaries

A background materials for the construction of Atangana–Baleanu derivative model, we supply some related results in the following:

Definition 1. Assume that $\Psi(t) \in \mathcal{H}^1(\zeta_1, \zeta_2)$, for $\zeta_2 > \zeta_1$, $0 \le \rho \le 1$, then the Atangana–Baleanu $\mathcal{ABC}$ derivative is defined by,

$$ {}^{\mathcal{ABC}}_{0}D^{\rho}_{t} g(t) = \frac{\mathcal{AB}(\rho)}{1-\rho} \int_b^t \frac{d}{d\xi} g(\xi) E_{\xi}\left[-\frac{\rho}{1-\rho}(t-\xi)^{\rho}\right] d\xi. \tag{10} $$

Definition 2. The integral for the derivative in (10) is

$$ {}^{\mathcal{ABC}}_{0}I^{\rho}_{t} g(t) = \frac{(1-\rho)}{\mathcal{AB}(\rho)} g(t) + \frac{\rho}{\mathcal{AB}(\rho)\Gamma(\rho)} \int_0^t (t-\xi)^{\rho-1} g(\xi) d\xi. \tag{11} $$

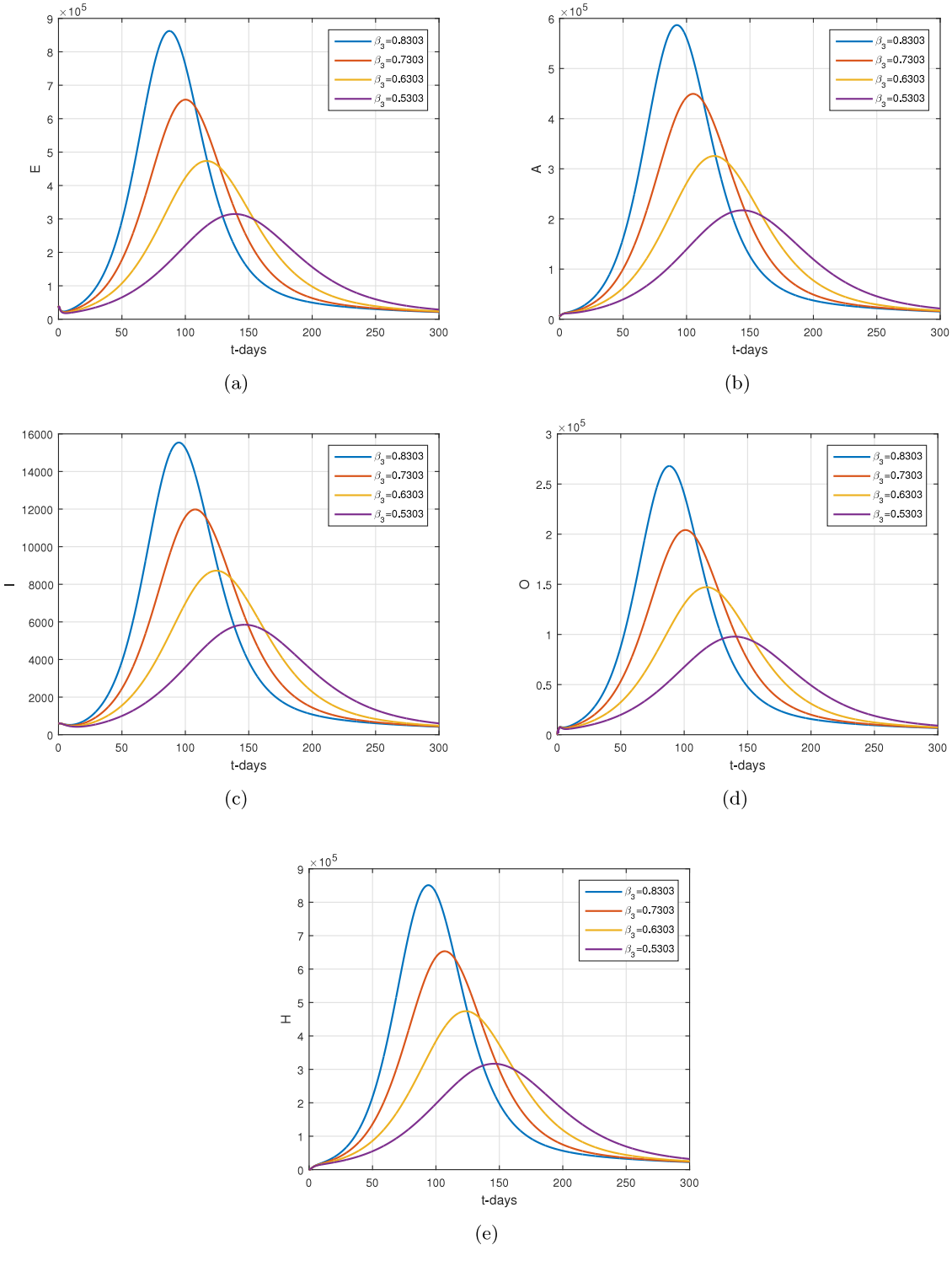

Fig. 4. The effect of β_3 on the infected compartments.

Omicron $\mathcal{ABC}$ model and its properties

We apply the definition of the Atangana–Baleanu derivative to the system (9), we then get the following generalized model:

$$\begin{cases} {}^{\mathcal{ABC}}_{0}\mathcal{D}_t^{\rho} S = \Lambda - (\mu + \lambda)S, \\ {}^{\mathcal{ABC}}_{0}\mathcal{D}_t^{\rho} E = \lambda S - Q_0 E, \\ {}^{\mathcal{ABC}}_{0}\mathcal{D}_t^{\rho} A = \delta\kappa E - Q_1 A, \\ {}^{\mathcal{ABC}}_{0}\mathcal{D}_t^{\rho} I = (1-\kappa-\phi)\delta E - Q_2 I, \\ {}^{\mathcal{ABC}}_{0}\mathcal{D}_t^{\rho} O = \phi\delta E - Q_3 O, \\ {}^{\mathcal{ABC}}_{0}\mathcal{D}_t^{\rho} H = q_1 I + q_2 O - Q_4 H, \end{cases} \tag{12}$$

where $\rho \in [0,1]$ defines the fractional order. The initial conditions for the system (12) are given by,

$$\begin{aligned} &{}^{\mathcal{ABC}}_{0}\mathcal{D}_t^{\rho} S(0) \geq 0, \quad {}^{\mathcal{ABC}}_{0}\mathcal{D}_t^{\rho} E(0) \geq 0, \quad {}^{\mathcal{ABC}}_{0}\mathcal{D}_t^{\rho} A(0) \geq 0, \\ &{}^{\mathcal{ABC}}_{0}\mathcal{D}_t^{\rho} I(0) \geq 0, \quad {}^{\mathcal{ABC}}_{0}\mathcal{D}_t^{\rho} O(0) \geq 0, \quad {}^{\mathcal{ABC}}_{0}\mathcal{D}_t^{\rho} H(0) \geq 0. \end{aligned} \tag{13}$$

We note that all the model parameters in (12) are non-negative. We define Ω to be the invariant region for our model equation and let

$$N(t) \leq N_{(0)}\mathcal{E}_{\rho,1}(-\mu t^{\rho}) + \pi t^{\rho}\mathcal{E}_{(\rho,\tau+1)}(-\mu t^{\rho}).$$

Then the biological feasible region for model (12) is given by

$$\Omega = \left\{ \Big(S(t), E(t), A(t), I(t), H(t)\Big) \in \mathbb{R}_+^5 : N(t) \leq \frac{\Lambda}{\mu}, \right.$$
$$\left. O(t) \in \mathbb{R}_+ : O(t) \leq \frac{\Lambda\phi\delta}{\mu Q_3} \right\}.$$

We establish the positivity of the fractional $\mathcal{ABC}$ model (12) solutions in the following:

Theorem 1. *For the initial conditions stated in (13) for every $t \geq 0$, the set Ω attracts all positive solutions associated to the model (12).*

Proof. It follows from the model (12) that

$$\begin{aligned} &{}^{\mathcal{ABC}}_{0}\mathcal{D}_t^{\rho} S|_{S=0} = \Lambda > 0, \\ &{}^{\mathcal{ABC}}_{0}\mathcal{D}_t^{\rho} E|_{E=0} = \frac{\beta_1 A + \beta_2 I + \beta_3 O + \beta_4 H}{N} \geq 0, \\ &{}^{\mathcal{ABC}}_{0}\mathcal{D}_t^{\rho} A|_{A=0} = \delta\kappa E \geq 0, \\ &{}^{\mathcal{ABC}}_{0}\mathcal{D}_t^{\rho} I|_{I=0} = (1-\kappa-\phi)\delta E \geq 0, \\ &{}^{\mathcal{ABC}}_{0}\mathcal{D}_t^{\rho} O|_{O=0} = \phi\delta E \geq 0, \\ &{}^{\mathcal{ABC}}_{0}\mathcal{D}_t^{\rho} H|_{H=0} = q_1 I + q_2 O \geq 0. \end{aligned} \tag{14}$$

Eq. (14) prove the positivity of solution with the initial conditions given in (13) remains in Ω for every $t \geq 0$. □

Mathematical analysis of the model

The purpose of this section is to explore the mathematical analysis of the model (12) based on their possible equilibrium points, that will be obtained in the following:

Disease-free equilibrium (DFE)

First, we find the disease-free equilibrium (DFE) of the model (12) denoted by E_0^* and can be obtained by using $E^* = A^* = I^* = O^* = H^* = 0$, Therefore, the DFE E_0^* is given by:

$$E_0^* = \left(S^*, E^*, A^*, I^*, O^*, H^*\right) = \left(\frac{\Lambda}{\mu}, 0, 0, 0, 0, 0\right).$$

The basic reproduction number

The basic reproduction number is an important threshold quantity which is useful to study the model stability at their equilibrium points. We follow [43] to compute the basic reproduction number of the model (12) denoted by $\mathcal{R}_0$. Here, $\mathcal{R}_0$ is defined to be the average number of new infections generated by an infectious individual during the course of disease progression by direct or indirect contact with a COVID-19 wholly susceptible population with a high possibility of having the Omicron variant causative agent. A next-generation matrix approach given in [43] can be used to get the basic reproduction number $\mathcal{R}_0$ for the system (12) as follows: The matrices F and V that define the new infections and transfer of the $\mathcal{ABC}$ model (12) respectively evaluated at the DFE and given by:

$$F = \begin{pmatrix} 0 & \beta_1 & \beta_2 & \beta_3 & \beta_4 \\ 0 & 0 & 0 & 0 & 0 \\ 0 & 0 & 0 & 0 & 0 \\ 0 & 0 & 0 & 0 & 0 \\ 0 & 0 & 0 & 0 & 0 \end{pmatrix} \text{ and}$$

$$V = \begin{pmatrix} Q_0 & 0 & 0 & 0 & 0 \\ -\delta\kappa & Q_1 & 0 & 0 & 0 \\ -(1-\kappa-\phi)\delta & 0 & Q_2 & 0 & 0 \\ -\phi\delta & 0 & 0 & Q_3 & 0 \\ 0 & 0 & -q_1 & -q_2 & Q_4 \end{pmatrix}.$$

$\mathcal{R}_0$ is the spectral radius of the matrix $\rho_1(FV^{-1})$, which is given by

$$\begin{aligned} \mathcal{R}_0 &= \rho_1(FV^{-1}) = \mathcal{R}_{0A} + \mathcal{R}_{0I} + \mathcal{R}_{0O} + \mathcal{R}_{0H}, \\ \mathcal{R}_0 &= \frac{\beta_1\delta\kappa}{Q_0 Q_1} + \frac{\beta_2\delta(1-\kappa-\phi)}{Q_0 Q_2} + \frac{\beta_3\delta\phi}{Q_0 Q_3} \\ &\quad + \frac{\beta_4\delta\left(\phi q_2 Q_2 + q_1 Q_3(1-\kappa-\phi)\right)}{Q_0 Q_2 Q_3 Q_4}. \end{aligned} \tag{15}$$

In expression (15), we have that $\mathcal{R}_{0A}$, $\mathcal{R}_{0I}$, $\mathcal{R}_{0H}$, $\mathcal{R}_{0O}$ are individual contributions to the $\mathcal{R}_0$ by A, I, O and H compartments respectively.

Endemic equilibrium

The model endemic equilibrium point is obtained by solving model (12) when the disease is at its endemic state. We therefore obtain the omicron endemic equilibrium denoted by $\mathfrak{E}_1^{**} = (S^{**}, E^{**}, A^{**}, I^{**}, O^{**}, H^{**})$ where

$$\begin{aligned} S^{**} &= \frac{Q_0 E^{**}}{\lambda^{**}} = \frac{\Lambda}{(\mu + \lambda^{**})}, \\ E^{**} &= \frac{\Lambda\lambda^{**}}{(\mu + \lambda^{**})Q_0}, \\ A^{**} &= Q_5 E^{**}, \\ I^{**} &= Q_6 E^{**}, \\ O^{**} &= Q_7 E^{**}, \\ H^{**} &= Q_8 E^{**}. \end{aligned} \tag{16}$$

In Eq. (16) we have that $Q_5 = \frac{\delta\kappa}{Q_1}$, $Q_6 = \frac{(1-\kappa-\phi)\delta}{Q_2}$, $Q_7 = \frac{\delta\phi}{Q_3}$, $Q_8 = \frac{(q_1 Q_6 + q_2 Q_7)}{Q_4}$ and

$$\lambda^{**} = \frac{\beta_1 A^{**} + \beta_2 I^{**} + \beta_3 O^{**} + \beta_4 H^{**}}{S^{**} + E^{**} + A^{**} + I^{**} + O^{**} + H^{**}} \tag{17}$$

Substituting (16) into (17) we get the

$$f(\lambda^{**}) = \varpi_1(\lambda^{**})^2 + \varpi_0(\lambda^{**}) = 0,$$

for

$$\begin{aligned} \varpi_0 &= \Lambda Q_0(1 - \mathcal{R}_0), \\ \varpi_1 &= \Lambda(Q_5 + Q_6 + Q_7 + Q_8). \end{aligned}$$

Clearly both ϖ_0 and ϖ_1 are positive whenever $\mathcal{R}_0 < 1$. The solution $\lambda^{**} = \frac{\varpi_0}{\varpi_1}$ is negative and hence we conclude that there is no endemic equilibrium if $\mathcal{R}_0 < 1$. Note that E^{**} exist if $\lambda^{**} > 0$ and when $\lambda^{**} = 0$ gives the DFE.

Stability of the DFE

We establish the stability results of the system (12) at the disease free case. The following theorems and their proof are given in details.

Theorem 2. *Consider that* $\ell_1, \ell_2 \in \mathscr{H}$ *such that* $gcd(\ell_1, \ell_2) = 1$ *and* $d = \frac{\ell_1}{\ell_2}$. *If* $\mathscr{M} = \ell_2$, *then, the DFE of the model* (12) *is locally asymptotically stable (LAS) if* $|arg(\chi)| > \frac{2\pi}{\mathscr{M}}$ *for every roots of* χ *of the characteristics Eq.* (18) *of the matrix* $\mathcal{J}_{(E_0^*)}$,

$$det\Big(diag\Big[\chi^{\ell_1}\chi^{\ell_1}\chi^{\ell_1}\chi^{\ell_1}\chi^{\ell_1}\Big]\Big) - \mathcal{J}_{E_0^*} = 0. \tag{18}$$

Proof. Evaluating the Jacobian matrix of system (12) gives the following matrix

$$\mathcal{J}_{E_0^*} = \begin{pmatrix} -\mu & 0 & -\beta_1 & -\beta_2 & -\beta_3 & -\beta_4 \\ 0 & -Q_0 & \beta_1 & \beta_2 & \beta_3 & \beta_4 \\ 0 & \delta\kappa & -Q_1 & 0 & 0 & 0 \\ 0 & -(1-\kappa-\phi)\delta & 0 & -Q_2 & 0 & 0 \\ 0 & \phi\delta & 0 & 0 & -Q_3 & 0 \\ 0 & 0 & 0 & q_1 & q_2 & -Q_4 \end{pmatrix}, \tag{19}$$

with the associated characteristics polynomial of $\mathcal{J}(E_0^*)$ given by

$$(\chi^{\ell_1} + \mu)\Big(\chi^{5\ell_1} + a_4\chi^{4\ell_1} + a_3\chi^{3\ell_1} + a_2\chi^{2\ell_1} + a_1\chi^{\ell_1} + a_0\Big) = 0. \tag{20}$$

The arguments of the root of the equation $(\chi^{\ell_1} + \mu)$ is

$$\arg(\Pi_k) = \frac{\pi}{\ell_1} + \frac{2\pi k}{\ell_1} > \frac{\pi}{\mathscr{M}} > \frac{\pi}{\mathscr{M}},$$

where $k = 0, 1, \ldots, (\ell_1 - 1)$. The eigenvalues of Eq. (20) consist of $-\mu$, and those obtained from the solutions of the polynomial,

$$P(\chi) = \Big(\chi^{5\ell_1} + a_4\chi^{4\ell_1} + a_3\chi^{3\ell_1} + a_2\chi^{2\ell_1} + a_1\chi^{\ell_1} + a_0\Big)$$

where

$$\begin{aligned}
a_0 &= Q_0Q_1Q_2Q_3Q_4\big(1-\mathcal{R}_0\big),\\
a_1 &= Q_1Q_2Q_3Q_4 + \beta_4\delta Q_1\Big(\phi q_2 + q_1(1-\kappa-\phi)\Big)\\
&\quad + Q_0Q_1Q_2Q_3\big(1-\mathcal{R}_{0A}Y_0\big) + Q_0Q_1Q_2Q_4\big(1-\mathcal{R}_{0I}Y_1\big)\\
&\quad + Q_0Q_1Q_3Q_4\big(1-\mathcal{R}_{0O}Y_2\big) + Q_0Q_2Q_3Q_4\big(1-\mathcal{R}_{0H}Y_3\big),\\
a_2 &= Q_1Q_2Q_3 + Q_0Q_1Q_4 + Q_0Q_2Q_4 + Q_1Q_2Q_4 + Q_0Q_3Q_4\\
&\quad + Q_2Q_3Q_4 + Q_0Q_1Q_2\big(1-\mathcal{R}_{0A}Y_4\big)\\
&\quad + Q_0Q_2Q_3\big(1-\mathcal{R}_{0I}Y_5\big) + Q_0Q_1Q_3\big(1-\mathcal{R}_{0O}Y_6\big)\\
&\quad + Q_1Q_3Q_4\big(1-\mathcal{R}_{0H}Q_0Q_2\big),\\
a_3 &= Q_1Q_2 + Q_2Q_4 + Q_1Q_3 + Q_2Q_3 + Q_0Q_4 + Q_1Q_4 + Q_2Q_4\\
&\quad + Q_0Q_1\big(1-\mathcal{R}_{0A}\big) + Q_0Q_2\big(1-\mathcal{R}_{0I}\big)\\
&\quad + Q_0Q_3\big(1-\mathcal{R}_{0O}\big),\\
a_4 &= (Q_0 + Q_1 + Q_2 + Q_3 + Q_4),
\end{aligned}$$

In the above expression

$$Y_0 = \frac{(Q_2(Q_3+Q_4)+Q_3)}{Q_2Q_3},\ Y_1 = \frac{(Q_1(Q_3+Q_4)+Q_3Q_4)}{Q_1Q_4},$$
$$Y_2 = \frac{(Q_1(Q_2+Q_4)+Q_2Q_4)}{Q_1Q_4},$$
$$Y_3 = (Q_1(Q_2+Q_4)+Q_2Q_4), Y_4 = \frac{(Q_2+Q_3+Q_4)}{Q_2},$$
$$Y_5 = \frac{(Q_1+Q_2+Q_4)}{Q_3}$$
$$\text{and } Y_6 = \frac{(Q_1+Q_2+Q_4)}{Q_1}.$$

All the constants $a_i > 0$ for $i = 1, 2, 3, 4$ are positive when $\mathcal{R}_0 < 1$. Therefore, following the Routh–Hurwitz criterion the function $P(\chi)$ have eigenvalues with negative real parts since $a_i > 0$ and $a_1a_2a_3 > a_3^2 + a_1^2a_4$. On the other hand, using the fact that $a_i > 0$ it can then be easily established that second condition of Routh–Hurwitz criterion $(a_1a_4 - a_5)(a_1a_4a_3 - a_3^2 - a_1^2a_4) > a_5(a_1a_2 - a_3)^2 + a_1a_5^2$ is satisfied which guarantees the stability of the DFE whenever $\mathcal{R}_0 < 1$. Hence, the conditions require for the eigenvalues of the characteristics equation $|arg(\chi)| > \frac{2\pi}{\mathcal{M}}$ holds. Thus, E_0^* is LAS if $\mathcal{R}_0 < 1$. □

Global stability of the DFE

We begin by stating the theorem which necessary for the global stability of E_0^*.

Theorem 3. *The model given in* (12) *at the DFE is globally asymptotically stable (GAS) whenever* $\mathcal{R}_0 \le 1$.

Proof. Assume a C^1 Lyapunov function defined by

$$\mathcal{L}(t) = E(t) + \eta_1 A(t) + \eta_2 I(t) + \eta_3 O(t) + \eta_4 H(t),$$

comprising of all the compartments that taking part in the disease spread directly, where the non-negative constants $\eta_1, \eta_2, \eta_3, \eta_4$ shall be determined. Then, the $\mathcal{ABC}$ derivative of $\mathcal{L}(t)$ gives

$$\begin{aligned}
{}^{0}{}^{\mathcal{ABC}}D_t^{\rho}\mathcal{L}(t) &= {}^{0}{}^{\mathcal{ABC}}D_t^{\rho}E(t) + \eta_1{}^{0}{}^{\mathcal{ABC}}D_t^{\rho}A(t) + \eta_2{}^{0}{}^{\mathcal{ABC}}D_t^{\rho}I(t)\\
&\quad + \eta_3{}^{0}{}^{\mathcal{ABC}}D_t^{\rho}O(t) + \eta_4{}^{0}{}^{\mathcal{ABC}}D_t^{\rho}H(t),\\
&= \Big(\lambda S - Q_0E\Big) + \eta_1\big(\delta\kappa E - Q_1A\big)\\
&\quad + \eta_2\big((1-\kappa-\phi)\delta E - Q_2I\big) + \eta_3\big(\phi\delta E - Q_3O\big)\\
&\quad + \eta_4\big(q_1I + q_2O - Q_4H\big),\\
&= \Big(\frac{\beta_1A + \beta_2I + \beta_3O + \beta_4HS}{N} - Q_0E\Big) + \eta_1\big(\delta\kappa E - Q_1A\big)\\
&\quad + \eta_2\big((1-\kappa-\phi)\delta E - Q_2I\big)\\
&\quad + \eta_3\big(\phi\delta E - Q_3O\big) + \eta_4\big(q_1I + q_2O - Q_4H\big),\\
&\le \Big(\beta_1 - \eta_1Q_1\Big)A + \Big(\beta_2 - \eta_2Q_2 + \eta_4q_1\Big)I\\
&\quad + \Big(\beta_3 - \eta_3Q_3 + \eta_4q_2\Big)O + \Big(\beta_4 - \eta_4Q_4\Big)H\\
&\quad + \Big(\eta_1\kappa\delta + \eta_2(1-\kappa-\phi) + \eta_3\phi\delta - Q_0\Big)E,
\end{aligned} \tag{21}$$

Setting the coefficients of H, A, O and I to zero, we solve for η_i for $i = 1, 2, \ldots, 4$, which yields

$$\eta_1 = \frac{\beta_1}{Q_1},\ \eta_2 = \frac{(\beta_4Q_4 + \beta_4q_1)}{Q_2Q_4}\ \eta_3 = \frac{(\beta_3Q_4 + \beta_4q_2)}{Q_3Q_4} \text{ and } \eta_4 = \frac{\beta_4}{Q_4}.$$

Upon substitution of η_i into the last term in expression (21) we obtain

$${}^{0}{}^{\mathcal{ABC}}D_t^{\rho}\mathcal{L}(t) \le Q_0\Big(\mathcal{R}_0 - 1\Big)E. \tag{22}$$

Therefore, whenever $\mathcal{R}_0 \le 1$, we have that ${}^{\mathcal{ABC}}D_t^{\rho}\mathcal{L}(t)$ is negative and zero if $\mathcal{R}_0 = 1$. Thus, using the result of LaSalle's invariant principle [44], the model at E_0^* is GAS in the invariant region. □

Existence and uniqueness of solutions

It is obvious that the model (12) is a highly nonlinear model and its exact solution is very difficult to its nonlinearity, so, the existence and uniqueness criteria will ensure that the model will solution exists and shall be unique. If possibly there may be a method developed in the future to solve the nonlinear model, then the existence and uniqueness criteria will ensure it. In order to do this, we apply the fixed point theory to have results of the existence and uniqueness of solutions of the system (12) in the following:

$$\begin{cases} {}_0^{\mathcal{ABC}}D_t^{\rho}\mathcal{F}(t) := \mathcal{G}(t, \mathcal{F}(t)), \\ \mathcal{F}(0) := \mathcal{F}_0, \text{ for } 0 < t < T < \infty \end{cases} \tag{23}$$

for $\mathcal{F}(t) = (S, E, A, I, O, H)$ and $\mathcal{G}$ been the continuous vector function defined by

$$\mathcal{G} = \begin{pmatrix} \mathcal{G}_1(\mathcal{X}) \\ \mathcal{G}_2(\mathcal{X}) \\ \mathcal{G}_3(\mathcal{X}) \\ \mathcal{G}_4(\mathcal{X}) \\ \mathcal{G}_5(\mathcal{X}) \\ \mathcal{G}_6(\mathcal{X}) \end{pmatrix} = \begin{pmatrix} \Lambda - (\mu + \lambda)S(t), \\ \lambda S(t) - Q_0 E(t), \\ \delta\kappa E(t) - Q_1 A(t), \\ (1 - \kappa - \phi)\delta E(t) - Q_2 I(t), \\ \phi\delta E(t) - Q_3 O(t), \\ q_1 I(t) + q_2 O(t) - Q_4 H(t), \end{pmatrix}. \tag{24}$$

with an initial conditions $\mathcal{G}_0(t) = \big(S(0), E(0), A(0), I(0), O(0), H(0)\big)$. The function $\mathcal{G}$ is said to satisfy Lipschitz conditions for uniform continuity stated below

$$\|\mathcal{G}(t, \mathcal{F}_1(t)) - \mathcal{G}(t, \mathcal{F}_2(t))\| \leq \quad \mathcal{M}\|\mathcal{F}_1(t) - \mathcal{F}_2(t)\|. \tag{25}$$

The theorem stated below that guarantees about the existence and uniqueness of the system (24).

Theorem 4. *Existence and uniqueness*

The fractional system (24) in $\mathcal{ABC}$ possess a unique solution if the condition in the following is satisfied,

$$\frac{(1-\rho)}{\mathcal{B}(\rho)} + \frac{\rho}{\mathcal{B}(\rho)r(\rho)} T^{\rho}_{max} < 1.$$

Proof. We apply the AB-integral on the system (23), and obtain the following:

$$\mathcal{F}(t) = \mathcal{F}_0 + \frac{(1-\rho)}{\mathcal{B}(\rho)}\rho(t, \mathcal{F}(t)) + \frac{\rho}{\mathcal{B}(\rho)r(\rho)} \int_0^t (t-\xi)\mathcal{G}(\xi, \mathcal{F}(\xi))d\xi. \tag{26}$$

Setting $\mathcal{J} = (0, T)$ and considering the operator $\Phi : C(\mathcal{J}, \mathbb{R}^6) \to C(\mathcal{J}, \mathbb{R}^6)$, which is defined by

$$\begin{aligned} \Phi(\mathcal{F}(t)) =& \mathcal{F}_0 + \frac{(1-\rho)}{\mathcal{B}(\rho)}\mathcal{G}(t, \mathcal{F}(t)) \\ &+ \frac{\rho}{\mathcal{B}(\rho)r(\rho)} \int_0^t (t-\xi)^{(\rho-1)}\rho(\xi, \mathcal{F}(\xi))d\xi \quad \square \end{aligned} \tag{27}$$

Eq. (26) yields

$$\mathcal{F}(t) = \Phi\big[\mathcal{F}(t)\big]. \tag{28}$$

Therefore, the supremum of $\mathcal{J}$, $\|.\|_{\mathcal{J}}$ is

$$\|\mathcal{F}(t)\|_{\mathcal{J}} = \sup_{t\in\mathcal{J}}\|\mathcal{F}(t)\|, \ \mathcal{F}(t) \in C$$

where $C(\mathcal{J}, \mathbb{R}^6)$ with the norm $\|.\|_{\mathcal{J}}$ represents the Banach space. Furthermore,

$$\left\| \int_0^t \mathcal{D}(t-\xi)\mathcal{F}(\xi)d\xi \right\| \leq \quad T\|\mathcal{D}(t,\xi)\|_{\mathcal{J}}\|\mathcal{F}(t)\|_{\mathcal{J}} \tag{29}$$

for $\mathcal{G}(t) \in C(\mathcal{J}, \mathbb{R}^5)$, $\mathcal{D}(t, z) \in C(\mathcal{J}^2, \mathbb{R}^6)$ so that

$$\|D(t, z)\|_J = \sup_{t,z\in\mathcal{J}}\|D(t, z)\|.$$

Upon employing Φ we get

$$\begin{aligned} \left\| \Big[\Phi(t, \mathcal{F}_1(t)) - \Phi(t, \mathcal{F}_2(t))\Big] \right\|_{\mathcal{J}} \leq \quad & \left\| \frac{(1-\rho)}{\mathcal{B}(\rho)}\mathcal{G}(t, \mathcal{F}_1(t)) - \mathcal{G}(t, \mathcal{F}_2(t)) \right. \\ & + \frac{\alpha}{\mathcal{B}(\alpha)\Gamma(\alpha)} \int_0^t (t-\xi)^{(\rho-1)} \\ & \left. \times \Big[\mathcal{G}(\xi, \mathcal{F}_1, \xi) - \mathcal{G}(\xi, \mathcal{F}_2, \xi)\Big] d\xi \right\| \end{aligned}$$

Applying the Lipschitz conditions in (25), results from (29) and combine with the principles of triangular inequality, we obtain:

$$\begin{aligned} \|\Phi(\mathcal{G}_1(t)) - \Phi(\mathcal{G}_2(t))\|_{\mathcal{J}} \leq \quad & \left[\frac{1-\rho}{\mathcal{B}(q)}\mathcal{G}(t, \mathcal{G}_1(t))\rho + \frac{\rho}{\mathcal{B}(\alpha)r(\rho)}\mathcal{B}T^{\rho}_{\max}\right] \\ & \int_0^t (t-\xi)^{q-1} \left\| \mathcal{G}_1(t) - \mathcal{G}_2(t) \right\|_{\mathcal{J}}. \end{aligned}$$

following some algebraic simplification. Hence,

$$\|\Phi(\mathcal{G}_1(t)) - \Phi(\mathcal{G}_2(t))\|_J \leq \quad \mathcal{B}\left\|\mathcal{G}_1(t) -_2 (t)\right\|_{\mathcal{J}}.$$

in which

$$\mathcal{B} = \frac{(1-\rho)}{\mathcal{B}(\rho)}\mathcal{M} + \frac{\rho}{\mathcal{B}(\alpha)r(\rho)}\mathcal{M}T^{\rho}_{\max}.$$

So, the operator Φ should be a contraction if the condition (25) satisfy $C(\mathcal{J}, \mathbb{R}^6)$. Conclusively, with the Banach fixed-point theorem our model (24) has a unique solutions and exist.

Model numerical scheme using $\mathcal{ABC}$

With the help of the Adams–Bashforth method shown in [45], we present a numerical algorithm for the solution of the omicron model (12). To achieve this, we re-write (23) as follows,

$$\begin{aligned} &{}^{\mathcal{ABC}}_{0}\mathcal{D}^{\rho}_t S(t) = \mathcal{H}_1(t, S, E, A, I, O, H), \\ &{}^{\mathcal{ABC}}_{0}\mathcal{D}^{\rho}_t E(t) = \mathcal{H}_2(t, S, E, A, I, O, H), \\ &{}^{\mathcal{ABC}}_{0}\mathcal{D}^{\rho}_t A(t) = \mathcal{H}_3(t, S, E, A, I, O, H), \\ &{}^{\mathcal{ABC}}_{0}\mathcal{D}^{\rho}_t I(t) = \mathcal{H}_4(t, S, E, A, I, O, H), \\ &{}^{\mathcal{ABC}}_{0}\mathcal{D}^{\rho}_t O(t) = \mathcal{H}_5(t, S, E, A, I, O, H), \\ &{}^{\mathcal{ABC}}_{0}\mathcal{D}^{\rho}_t H(t) = \mathcal{H}_6(t, S, E, A, I, O, H). \end{aligned} \tag{30}$$

Next, we convert Eq. (30) into a Volterra type integral considering the fundamental theorem of fractional calculus, which yields

$$\begin{aligned} S(t_{k+1}) = \quad & S(0) + \frac{1-\rho}{\mathcal{ABC}(\rho)}\mathcal{H}_1(t_k, S) + \frac{\rho}{\mathcal{ABC}(\rho)\Gamma(\rho)} \\ & \times \sum_{t_j=0}^{k} \int_{t_j}^{t_{j+1}} (t_{k+1} - \xi)^{\rho-1}\mathcal{H}_1(\xi, S)d\xi \\ E(t_{k+1}) = \quad & E(0) + \frac{1-\rho}{\mathcal{ABC}(\rho)}\mathcal{H}_2(t_k, E) + \frac{\rho}{\mathcal{ABC}(\rho)\Gamma(\rho)} \\ & \times \sum_{t_j=0}^{k} \int_{t_j}^{t_{j+1}} (t_{k+1} - \xi)^{\rho-1}\mathcal{H}_2(\xi, E)d\xi, \\ A(t_{k+1}) = \quad & A(0) + \frac{1-\rho}{\mathcal{ABC}(\rho)}\mathcal{H}_3(t_k, A) + \frac{\rho}{\mathcal{ABC}(\rho)\Gamma(\rho)} \\ & \times \sum_{t_j=0}^{k} \int_{t_j}^{t_{j+1}} (t_{k+1} - \xi)^{\rho-1}\mathcal{H}_3(\xi, A)d\xi \\ I(t_{k+1}) = \quad & I(0) + \frac{1-\rho}{\mathcal{ABC}(\rho)}\mathcal{H}_4(t_k, I) + \frac{\rho}{\mathcal{ABC}(\rho)\Gamma(\rho)} \\ & \times \sum_{t_j=0}^{k} \int_{t_j}^{t_{j+1}} (t_{k+1} - \xi)^{\rho-1}\mathcal{H}_4(\xi, I)d\xi, \\ O(t_{k+1}) = \quad & O(0) + \frac{1-\rho}{\mathcal{ABC}(\rho)}\mathcal{H}_5(t_k, O) + \frac{\rho}{\mathcal{ABC}(\rho)\Gamma(\rho)} \\ & \times \sum_{t_j=0}^{k} \int_{t_j}^{t_{j+1}} (t_{k+1} - \xi)^{\rho-1}\mathcal{H}_5(\xi, O)d\xi, \\ H(t_{k+1}) = \quad & H(0) + \frac{1-\rho}{\mathcal{ABC}(\rho)}\mathcal{H}_6(t_k, H) + \frac{\rho}{\mathcal{ABC}(\rho)\Gamma(\rho)} \\ & \times \sum_{t_j=0}^{k} \int_{t_j}^{t_{j+1}} (t_{k+1} - \xi)^{\rho-1}\mathcal{H}_6(\xi, H)d\xi, \end{aligned} \tag{31}$$

It is of great importance to note that all the integrals in Eq. (31) were approximated using the interpolation polynomial and hence provides

the numerical scheme for the Omicron model (12). After some algebraic manipulation, finally, we get the numerical scheme for each compartment of the model:

$$
\begin{aligned}
S(t_{k+1}) = \; & S(0) + \frac{1-\rho}{\mathcal{ABC}(\rho)}\mathcal{H}_1(t_k, S) \\
& + \frac{\rho}{\mathcal{ABC}(\rho)\Gamma(\rho)}\sum_{t_j=0}^{k}\left[\frac{h^\rho \mathcal{H}_1(t_j, S)}{\Gamma(\rho+2)}(k+1-j)^\rho(k-j+2+\rho)\right. \\
& -(k-j)^\rho(k-j+2+2\rho) \\
& \left. -\frac{h^\rho \mathcal{H}_1(t_j, S)}{\Gamma(\rho+2)}\Big((k+1-j)^{\rho+1}-(k-j)^\rho(k-j+1+\rho)\Big)\right], \\
E(t_{k+1}) = \; & E(0) + \frac{1-\rho}{\mathcal{ABC}(\rho)}\mathcal{H}_2(t_k, E) \\
& + \frac{\rho}{\mathcal{ABC}(\rho)\Gamma(\rho)}\sum_{t_j=0}^{k}\left[\frac{h^\rho \mathcal{H}_2(t_j, E)}{\Gamma(\rho+2)}(k+1-j)^\rho(k-j+2+\rho)\right. \\
& -(k-j)^\rho(k-j+2+2\rho) \\
& \left. -\frac{h^\rho \mathcal{H}_2(t_j, E)}{\Gamma(\rho+2)}\Big((k+1-j)^{\rho+1}-(k-j)^\rho(k-j+1+\rho)\Big)\right], \\
A(t_{k+1}) = \; & A(0) + \frac{1-\rho}{\mathcal{ABC}(\rho)}\mathcal{H}_3(t_k, A) \\
& + \frac{\rho}{\mathcal{ABC}(\rho)\Gamma(\rho)}\sum_{t_j=0}^{k}\left[\frac{h^\rho \mathcal{H}_3(t_j, A)}{\Gamma(\rho+2)}(k+1-j)^\rho(k-j+2+\rho)\right. \\
& -(k-j)^\rho(k-j+2+2\rho) \\
& \left. -\frac{h^\rho \mathcal{H}_3(t_j, A)}{\Gamma(\rho+2)}\Big((k+1-j)^{\rho+1}-(k-j)^\rho(k-j+1+\rho)\Big)\right], \\
I(t_{k+1}) = \; & I(0) + \frac{1-\rho}{\mathcal{ABC}(\rho)}\mathcal{H}_4(t_k, I) \\
& + \frac{\rho}{\mathcal{ABC}(\rho)\Gamma(\rho)}\sum_{t_j=0}^{k}\left[\frac{h^\rho \mathcal{H}_4(t_j, I)}{\Gamma(\rho+2)}(k+1-j)^\rho(k-j+2+\rho)\right. \\
& -(k-j)^\rho(k-j+2+2\rho) \\
& \left. -\frac{h^\rho \mathcal{H}_4(t_j, I)}{\Gamma(\rho+2)}\Big((k+1-j)^{\rho+1}-(k-j)^\rho(k-j+1+\rho)\Big)\right], \\
O(t_{k+1}) = \; & O(0) + \frac{1-\rho}{\mathcal{ABC}(\rho)}\mathcal{H}_5(t_k, O) \\
& + \frac{\rho}{\mathcal{ABC}(\rho)\Gamma(\rho)}\sum_{t_j=0}^{k}\left[\frac{h^\rho \mathcal{H}_5(t_j, O)}{\Gamma(\rho+2)}(k+1-j)^\rho(k-j+2+\rho)\right. \\
& -(k-j)^\rho(k-j+2+2\rho) \\
& \left. -\frac{h^\rho \mathcal{H}_5(t_j, O)}{\Gamma(\rho+2)}\Big((k+1-j)^{\rho+1}-(k-j)^\rho(k-j+1+\rho)\Big)\right], \\
H(t_{k+1}) = \; & H(0) + \frac{1-\rho}{\mathcal{ABC}(\rho)}\mathcal{H}_6(t_k, H) \\
& + \frac{\rho}{\mathcal{ABC}(\rho)\Gamma(\rho)}\sum_{t_j=0}^{k}\left[\frac{h^\rho \mathcal{H}_6(t_j, H)}{\Gamma(\rho+2)}(k+1-j)^\rho(k-j+2+\rho)\right. \\
& -(k-j)^\rho(k-j+2+2\rho) \\
& \left. -\frac{h^\rho \mathcal{H}_6(t_j, H)}{\Gamma(\rho+2)}\Big((k+1-j)^{\rho+1}-(k-j)^\rho(k-j+1+\rho)\Big)\right],
\end{aligned}
\tag{32}
$$

for our $\mathcal{ABC}$ model. The numerical scheme presented (32) is now used to simulate our model in the next section with ρ as the $\mathcal{ABC}$ operator over the modeling time.

Piecewise model

This section study the model with piecewise differential equations. The piecewise differential equation model is useful when there is multi-layer data which is not easy to obtained their fitting with the ordinary differential equation. So, the piecewise modeling approach is novel and recently reported to obtain reasonable analysis of epidemic models as well as other physical problems. We extend the model (9) into piecewise differential equations given by

$$
\begin{cases}
\frac{dS}{dt} = \Lambda - (\mu+\lambda)S, \\
\frac{dE}{dt} = \lambda S - Q_0 E, \\
\frac{dA}{dt} = \delta\kappa E - Q_1 A, \\
\frac{dI}{dt} = (1-\kappa-\phi)\delta E - Q_2 I, \\
\frac{dO}{dt} = \phi\delta E - Q_3 O, \\
\frac{dH}{dt} = q_1 I + q_2 O - Q_4 H, \\
\frac{dR}{dt} = \psi_1 A + \psi_2 I + \psi_3 O + \psi_4 H - \mu R.
\end{cases}
\tag{33}
$$

In model (33), we use $0 \le t < T_1$. When $T_1 \le t < T_2$, we give the following model:

$$
\begin{cases}
{}^{ABC}_{0}D_t^\rho S = \Lambda - (\mu+\lambda)S, \\
{}^{ABC}_{0}D_t^\rho E = \lambda S - Q_0 E, \\
{}^{ABC}_{0}D_t^\rho A = \delta\kappa E - Q_1 A, \\
{}^{ABC}_{0}D_t^\rho I = (1-\kappa-\phi)\delta E - Q_2 I, \\
{}^{ABC}_{0}D_t^\rho O = \phi\delta E - Q_3 O, \\
{}^{ABC}_{0}D_t^\rho H = q_1 I + q_2 O - Q_4 H, \\
{}^{ABC}_{0}D_t^\rho R = \psi_1 A + \psi_2 I + \psi_3 O + \psi_4 H - \mu R.
\end{cases}
\tag{34}
$$

When $T_2 \le t \le T$, we give the following model:

$$
\begin{cases}
dS = (\Lambda - (\mu+\lambda)S + \sigma_1 S dB_1(t), \\
\frac{dE}{dt} = \lambda S - Q_0 E) + \sigma_2 E dB_2(t), \\
dA = (\delta\kappa E - Q_1 A) + \sigma_3 A dB_3(t), \\
dI = ((1-\kappa-\phi)\delta E - Q_2 I) + \sigma_4 dB_4(t), \\
dO = (\phi\delta E - Q_3 O) + \sigma_5 O dB_5(t), \\
dH = (q_1 I + q_2 O - Q_4 H) + \sigma_6 H dB_6(t), \\
dR = (\psi_1 A + \psi_2 I + \psi_3 O + \psi_4 H - \mu R) + \sigma_7 R dB_7(t).
\end{cases}
\tag{35}
$$

Here σ_l for $l = 1, \ldots, 7$ denotes the intensity constants of the stochastic environment and $B_l(t)$ for $l = 1, \ldots, 6$ are the standard Brownian motion. Next, we consider an efficient numerical approach to solve numerically the piecewise system using the approach given in details in the following:

$$
\begin{cases}
\frac{dU_i(t)}{dt} = f\left(t, U_i\right), \text{ if } 0 \le t \le T_1 \\
U_i(0) = U_{i,0}, i = 1, 2, \ldots, n \\
{}_{T_1}{}^{ABC}D_t^\rho U_i(t) = f\left(t, U_i\right), \text{ if } T_1 \le t \le T_2 \\
U_i\left(T_1\right) = U_{i,1}, \\
dU_i(t) = f\left(t, U_i\right)dt + \sigma_l U_i dB_i(t), \text{ if } T_2 \le t \le T \\
U_i\left(T_2\right) = U_{i,2}.
\end{cases}
\tag{36}
$$

The numerical scheme considered here is basically comes from [46,46, 47] and the application of this scheme can be seen in [48]. According to this rule, we divide $[0, T]$ into the following,

$$
\begin{aligned}
& 0 \le t_0 \le t_1 \le \cdots \le t_{m_1} \\
& = T_1 \le t_{m_1+1} \le t_{m_1+2} \le \cdots \le t_{m_2} = T_2 \le t_{m_2+1} \le t_{m_2+2} \le \cdots \le t_{m_3} = T.
\end{aligned}
$$

After some algebraic manipulations, we obtain the final scheme given by the following:

$$
\begin{aligned}
U_i^{n_1} = & U_i(0) + \sum_{j_1=2}^{n_1}\left[\frac{23}{12}f\left(t_{j_1}, U_{j_1}\right) - \frac{4}{3}f\left(t_{j_1-1}, U_{j_1-1}\right)\right. \\
& \left. + \frac{5}{12}f\left(t_{j_1-2}, U_{j_1-2}\right)\right]\Delta t, 0 \le t \le T_1
\end{aligned}
$$

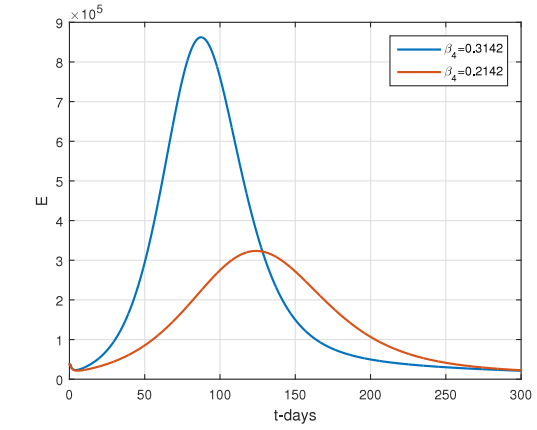

(a)

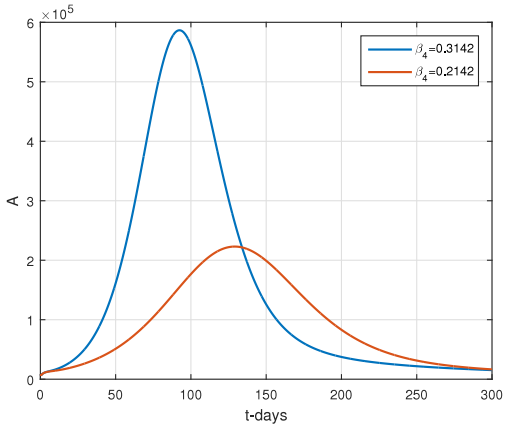

(b)

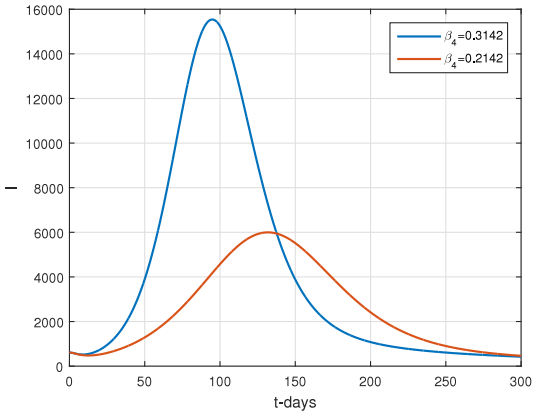

(c)

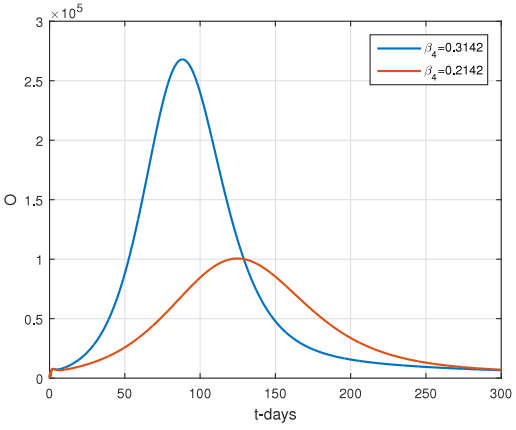

(d)

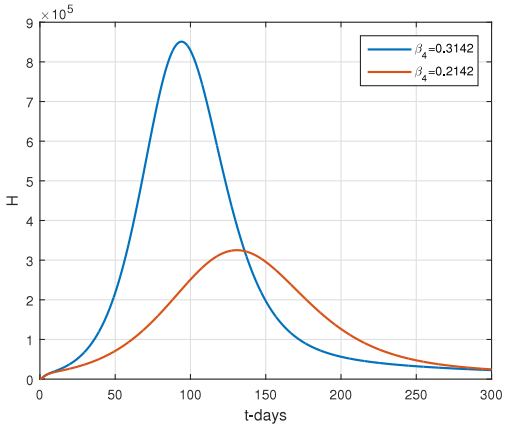

(e)

Fig. 5. The effect of β_4 on the infected compartments.

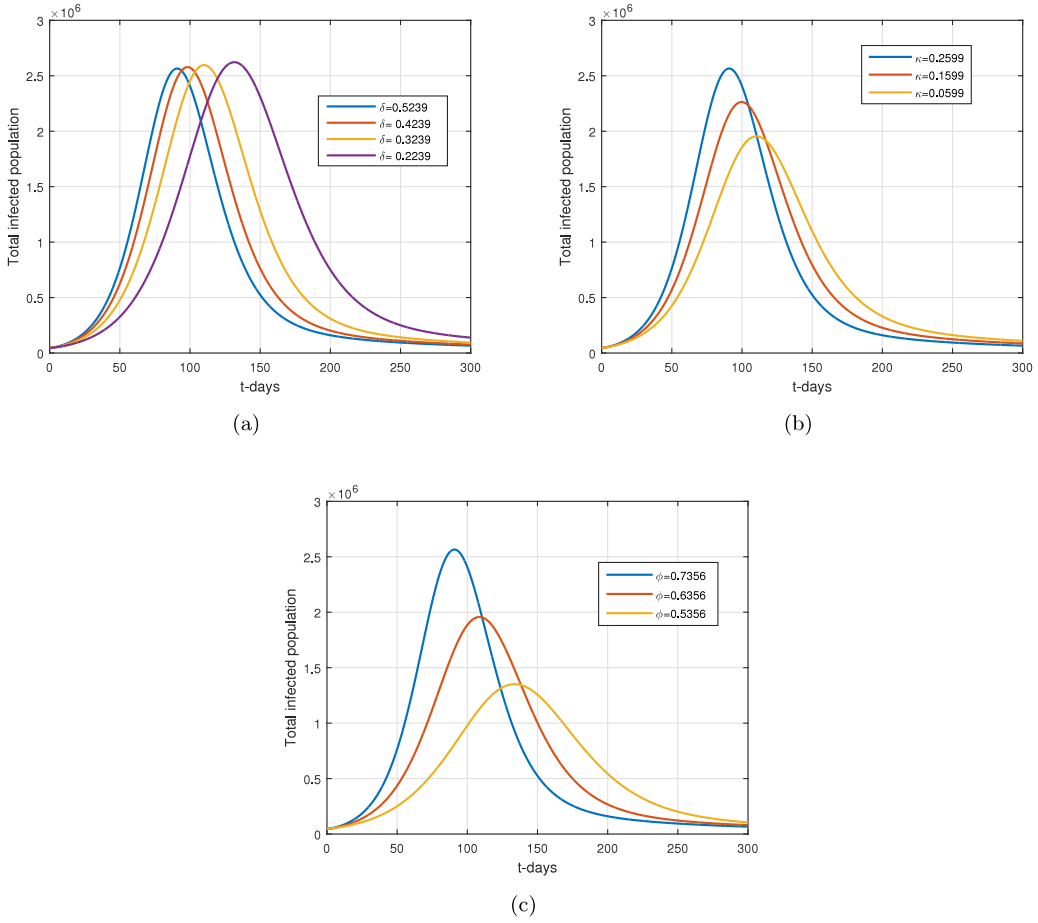

Fig. 6. The effect of δ, κ and ϕ on the infected compartments.

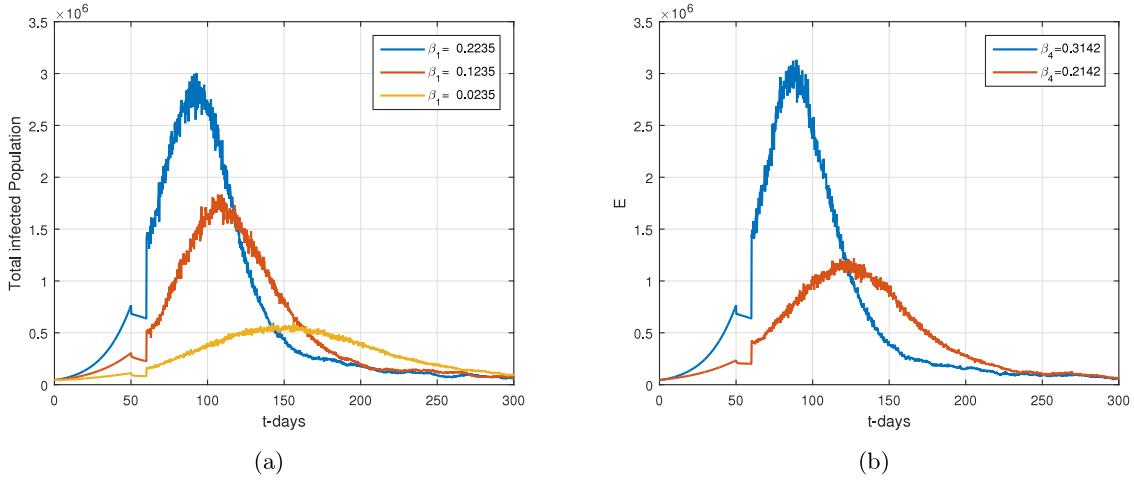

Fig. 7. The total infected population with $T_1 = 50$, $T_2 = 60$, $T_3 = 100$, $\sigma 1 = \sigma_2 = 0.1$, $\sigma_3 = \sigma_4 = \sigma_5 = \sigma_6 = \sigma_7 = 0.01$ and various value of β_1 and β_4.

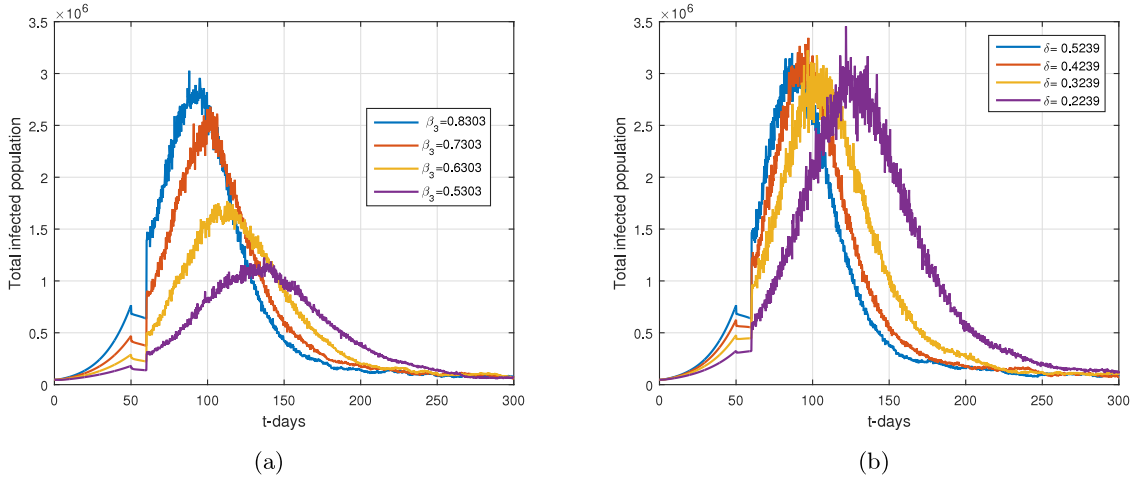

Fig. 8. The total infected population with $T_1 = 50$, $T_2 = 60$, $T_3 = 100$, $\sigma 1 = \sigma_2 = 0.1$, $\sigma_3 = \sigma_4 = \sigma_5 = \sigma_6 = \sigma_7 = 0.01$ and various value of β_3 and δ.

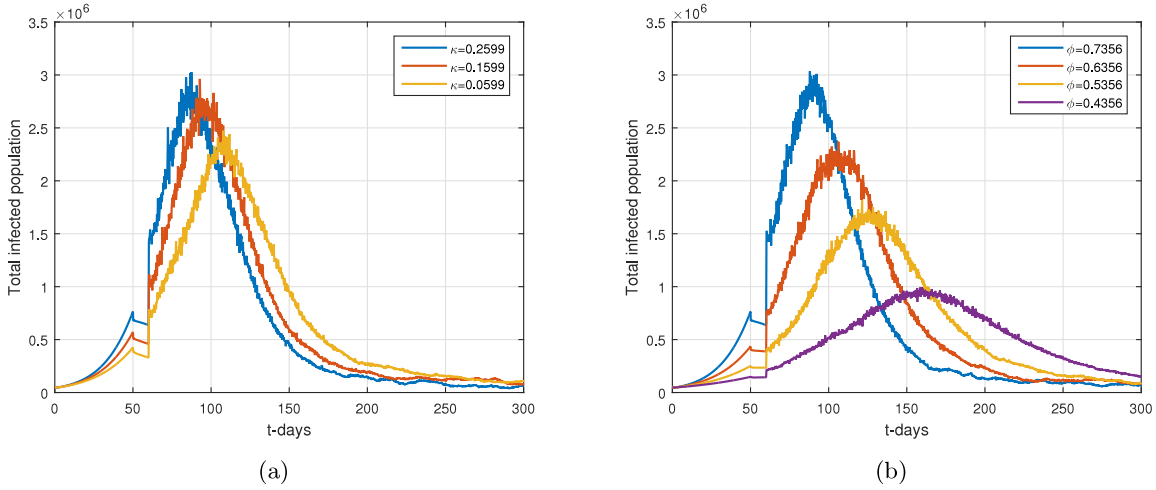

Fig. 9. The total infected population with $T_1 = 50$, $T_2 = 60$, $T_3 = 100$, $\sigma 1 = \sigma_2 = 0.1$, $\sigma_3 = \sigma_4 = \sigma_5 = \sigma_6 = \sigma_7 = 0.01$ and various value of κ and ϕ.

$$
\begin{aligned}
U_i^{n_2} =& U_i\left(T_1\right) + \frac{1-\rho}{AB(\rho)} f\left(t_{n_2}, U_{n_2}\right) + \frac{\rho(\Delta t)^\rho}{AB(\rho)\Gamma(\rho+1)} \\
&\times \sum_{j_2=n_1+3}^{n_2} f\left(t_{j_2-2}, U_{j_2-2}\right) K_1 \\
&+ \frac{\rho(\Delta t)^\rho}{AB(\rho)\Gamma(\rho+2)} \sum_{j_2=n_1+3}^{n_2} \left[f\left(t_{j_2-1}, U_{j_2-1}\right) - f\left(t_{j_2-2}, U_{j_2-2}\right)\right] K_2 \\
&+ \frac{\rho(\Delta t)^\rho}{2AB(\rho)\Gamma(\rho+3)} \sum_{j_2=n_1+3}^{n_2} \left[f\left(t_{j_2}, X_{j_2}\right) - 2f\left(t_{j_2-1}, X_{j_2-1}\right)\right. \\
&\left. + f\left(t_{j_2-2}, X_{j_2-2}\right)\right] K_3, \\
& T_1 \le t \le T_2,
\end{aligned}
\tag{37}
$$

$$
\begin{aligned}
U_i^{n_3} =& U_i\left(T_2\right) + \sum_{j_3=n_2+3}^{n_3} \left[\frac{23}{12} f\left(t_{j_3}, U_{j_3}\right) - \frac{4}{3} f\left(t_{j_3-1}, U_{j_3-1}\right)\right. \\
&\left. + \frac{5}{12} f\left(t_{j_3-2}, U_{j_3-2}\right)\right] \Delta t \\
&+ \sigma_l \sum_{j=n_2+3}^{n_3} U_i^{j_3} \left(B_l^{j_3} - B_l^{j_3-1}\right), T_2 \le t \le T,
\end{aligned}
$$

where

$$
\begin{aligned}
K_1 &= \left[\left(n_2 - j_2 + 1\right)^\rho - \left(n_2 - j_2\right)^\rho\right], \\
K_2 &= \left\{\begin{array}{l} \left(n_2 - j_2 + 1\right)^\rho \left(n_2 - j_2 + 3 + 2\rho\right) \\ -\left(n_2 - j_2\right)^\rho \left(n_2 - j_2 + 3 + 3\rho\right) \end{array}\right\}, \\
K_3 &= \left\{\begin{array}{l} \left(n_2 - j_2 + 1\right)^\rho \left[\begin{array}{c} 2\left(n_2 - j_2\right)^2 + (3\rho + 10)\left(n_2 - j_2\right) \\ +2\rho^2 + 9\rho + 12 \end{array}\right] \\ -\left(n_2 - j_2\right)^\rho \left[\begin{array}{c} 2\left(n_2 - j_2\right)^2 + (5\rho + 10)\left(n_2 - j_2\right) \\ +6\rho^2 + 18\rho + 10 \end{array}\right] \end{array}\right\}.
\end{aligned}
$$

Numerical simulation

This section studies the parameter estimations of the model (9) and their numerical solution. We consider the reported cases of COVID-19 infection in South Africa from March 202 to September 2021. These cases are taken from [49] on daily basis, so we consider the time unit *per day*. We consider the total population of South Africa in 2021 to be $N(0) = 60\,140\,000$, where the other variables of the model with their initial conditions are estimated to be $S(0) = 60\,093\,251$, $E(0) = 40\,000$, $A(0) = 6000$, $I(0) = 599$, $O(0) = 100$, $H(0) = 50$ and $R(0) = 0$. Among the model parameters, some of them are estimated, such as the average life expectancy in South Africa per day is $(1/(64.38 * 365))$ and the birth rate is obtained through the relation $\Lambda = \mu N(0) \approx 2559$. The estimated and fitted parameters obtained after the data fitting to the model (9)

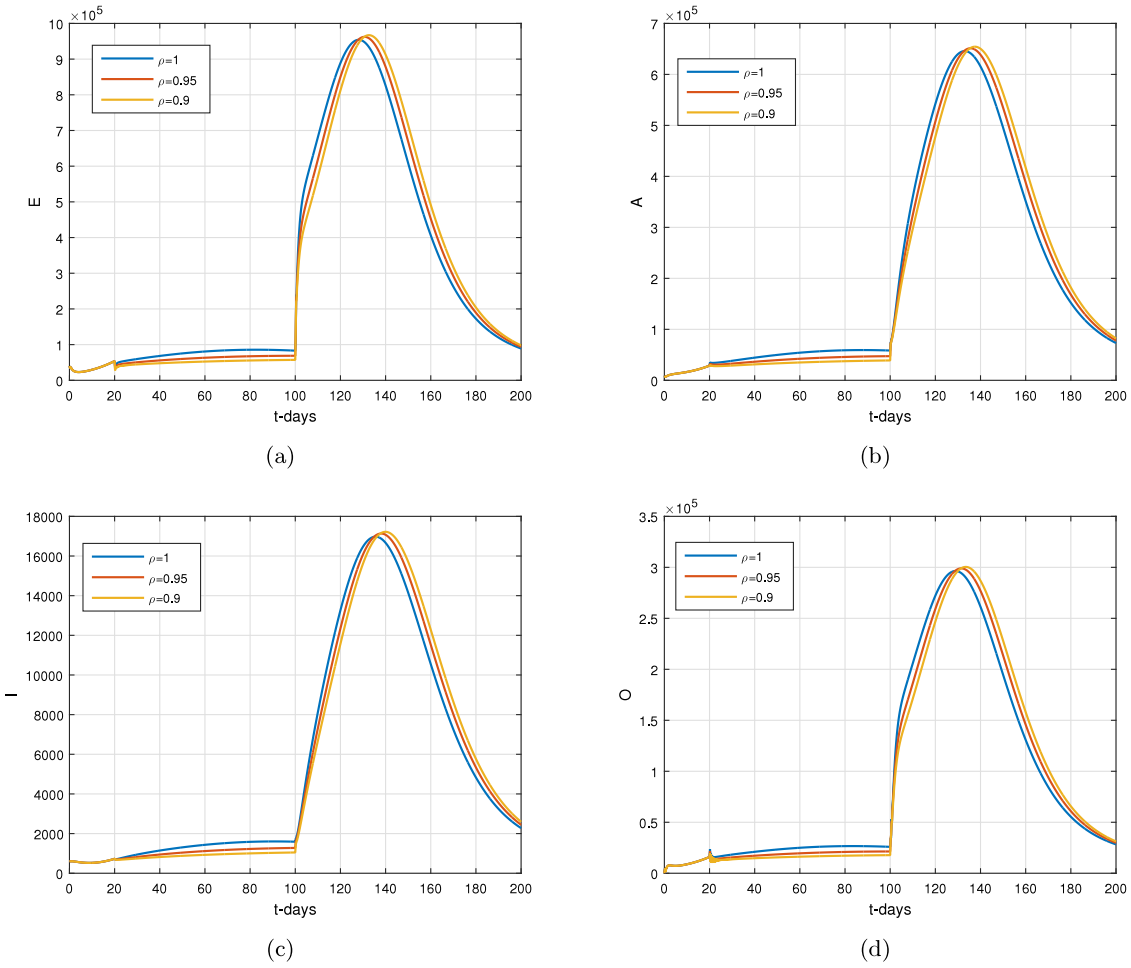

Fig. 10. The behavior of the fractional AB model for different value of ρ.

using the nonlinear least-square fitting are given in Table 1, while the fitting of the data to the model is given in 2. We performed the experiments until the desired fitting is obtained. The data is and their fitting show good agreement with each other. The basic reproduction number obtained approximately $\mathcal{R}_0 \approx 1.4004$.

Numerical results

We solve the model (9) using the values of the parameters shown in Table 1 and obtain the graphical results given in Figs. 3–6. In Fig. 3, taking into account the infected populations and obtain their graphical results with the variations on β_1. We observe if the individuals maintain social distances, wear face masks, avoid social gatherings, etc, the number of cases decreases, and also, in the future the cases will be less. The parameter β_3 with different variations decrease better the infected population, see 4. Decreasing the contact between the healthy and the hospitalized individuals can better decrease the population of infected individuals, see Fig. 5. The proportion of exposed individuals and their distribution upon the successful completion of their incubations decrease will the infective populations, see for details Fig. 6. One of the most important features of the omicron virus, is the past spreading among individuals, whether the individuals show disease symptoms or not, or if it is vaccinated or not. So, careful attention is required from the Government agencies, and the community help to decrease the infected cases while following the standard procedures suggested by World Health Organization (WHO). We simulate the piecewise model given in (33)–(35) using the same initial conditions and the values of the parameters and obtain some of the graphical solutions for it using the scheme obtained in (37), see Figs. 7–9. Fig. 7 shows the graphical solution of the piecewise model of the total infected compartments in the presence of the stochastic noises for different values of β_1 and β_4. It can be observe that the decrease in the value of β_1 and β_4, there is obviously decrease in the number of total infected cases very faster. In other words, the contact among the asymptomatic and hospitalized with healthy people can decrease the infected cases while maintaining the social distances, using face masks, getting the vaccine, etc. Similarly, the impact of the parameters β_3, δ, κ and ϕ also contribute in infection reduction of the total infected cases, see respectively Figs. 8 and 9. The behavior of the infected compartment of the Atangana–Baleanu model for different values of ρ is been given in Fig. 10.

Conclusion

We presented a new mathematical model for SARS-CoV-2 with an omicron variant. We formulated the model by using the assumptions of the omicron variant in the presence of hospitalized individuals. The classical model is extended to Atangana–Baleanu differential equation model and presented their mathematical results in detail. We studied the local and global asymptotical results for the omicron model when $\mathcal{R}_0 < 1$ (local asymptotical stability disease-free case), and $\mathcal{R}_0 \leq 1$ (global asymptotical stability disease free case). We studied the existence and uniqueness of the solution of the Atangana–Baleanu model. A numerical scheme to solve the Atangana–Baleanu model has been given in detail. Further, we used the new concept of the piecewise stochastic fractional differential equations which was recently reported

has been used to extend the model into the piecewise fractional stochastic Atangana–Baleanu stochastic differential equation model. A useful algorithm to solve the piecewise model has been given. Considering the reported cases of the COVID-19 in South Africa, we obtained the estimation of the parameters using the least-square fitting. We solved the model with the Atangana–Baleanu derivative and with a piecewise differential equation model numerically and presented a number of graphical results. The graphical results suggest that infection in South Africa with the Omicron variant can be minimized if the individuals in the community follow the recommendations of the WHO and also use the vaccinations.

CRediT authorship contribution statement

Xiao-Ping Li: Investigation, Validation, Writing – reviewing and editing. **Mahmoud H. DarAssi:** Investigation, Validation, Writing – reviewing and editing. **Muhammad Altaf Khan:** Conceptualization, Methodology, Software, Data curation, Writing – original draft, Visualization, Investigation, Validation, Writing – reviewing and editing. **C.W. Chukwu:** Conceptualization, Methodology, Software, Data curation, Writing – original draft, Visualization, Investigation, Validation, Writing – reviewing and editing. **Mohammad Y. Alshahrani:** Investigation, Validation, Writing – reviewing and editing. **Mesfer Al Shahrani:** Investigation, Validation, Writing – reviewing and editing, Visualization. **Muhammad Bilal Riaz:** Investigation Validation, Writing – reviewing and editing, Visualization.

Declaration of competing interest

The authors declare that they have no known competing financial interests or personal relationships that could have appeared to influence the work reported in this paper.

Acknowledgments

The authors extend their appreciation to the Deanship of Scientific Research at King Khalid University, Abha, Saudi Arabia for funding this work through general research groups program under grant number 53-40. This work was supported by the Key Scientific Research Projects of Hunan Provincial Department of Education in 2021 (Grant. No. 21A0525) and the Construction Project of Applied Characteristic Disciplines of Xiangnan University.

References

[1] Mohan BS, Nambiar V. Covid-19: An insight into sars-cov-2 pandemic originated at wuhan city in hubei province of china. J Infect Dis Epidemiol 2020;6(4):146.
[2] Coronavirus (covid-19) vaccinations. 2022, https://ourworldindata.org/covid-vaccinations, accessed 03/29/22.
[3] https://cals.ncsu.edu/applied-ecology/news/a-primer-on-coronavirus-variants-mutation-and-evolution/, accessed 03/29/22.
[4] Riddell Shane, Goldie Sarah, Hill Andrew, Eagles Debbie, Drew Trevor W. The effect of temperature on persistence of sars-cov-2 on common surfaces. Virol J 2020;17(1):1–7.
[5] https://www.nature.com/articles/d41586-022-00428-5, accessed 03/29/22.
[6] Centeres for disease control, cdc, potential rapid increase of omicron variant infections in the united states. 2022, https://www.cdc.gov/coronavirus/2019-ncov/science/forecasting/mathematical-modeling-outbreak.html, accessed 03/29/22.
[7] Who, world health organization. 2022, https://www.who.int/news/item/28-11-2021-update-on-omicron, accessed 03/29/22.
[8] Wang Bin-Guo, Wang Zhi-Cheng, Wu Yan, Xiong Yongping, Zhang Jiangqian, Ma Zhihui. A mathematical model reveals the influence of npis and vaccination on sars-cov-2 omicron variant. 2022.
[9] Aba Oud Mohammed A, Ali Aatif, Alrabaiah Hussam, Ullah Saif, Khan Muhammad Altaf, Islam Saeed. A fractional order mathematical model for covid-19 dynamics with quarantine, isolation, and environmental viral load. Adv Difference Equ 2021;2021(1):1–19.
[10] Chukwu CW, et al. Modelling fractional-order dynamics of covid-19 with environmental transmission and vaccination: A case study of indonesia. AIMS Math 2022;7(3):4416–38.
[11] Dar Assi Mahmoud H, Safi Mohammad A, Khan Muhammad Altaf, Beigi Alireza, Aly Ayman A, Alshahrani Mohammad Y. A mathematical model for sars-cov-2 in variable-order fractional derivative. Eur Phys J Spec Top 2022;1–10.
[12] Keeling Matt J, Brooks-Pollock Ellen, Challen Robert J, Danon Leon, Dyson Louise, Gog Julia Rose, Guzman-Rincon Laura, Hill Edward M, Pellis Lorenzo M, Read Jonathan M, et al. Short-term projections based on early omicron variant dynamics in England. medRxiv; 2021.
[13] Özköse Fatma, Yavuz Mehme, Şenel M Tamer, Habbireeh Rafla. Fractional order modelling of omicron sars-cov-2 variant containing heart attack effect using real data from the united kingdom. Chaos Solitons Fractals 2022;157:111954.
[14] Muniyappan Ashwin, Sundarappan Balamuralitharan, Manoharan Poongodi, Hamdi Mounir, Raahemifar Kaamran, Bourouis Sami, Varadarajan Vijayakumar. Stability and numerical solutions of second wave mathematical modeling on covid-19 and omicron outbreak strategy of pandemic: Analytical and error analysis of approximate series solutions by using hpm. Mathematics 2022;10(3):343.
[15] Nyabadza Farai, Chirove Faraimunashe, Chukwu CW, Visaya Maria Vivien. Modelling the potential impact of social distancing on the covid-19 epidemic in south africa. Comput Math Methods Med 2020;2020.
[16] Shen Zhong-Hua, Chu Yu-Ming, Khan Muhammad Altaf, Muhammad Shabbir, Al-Hartomy Omar A, Higazy M. Mathematical modeling and optimal control of the covid-19 dynamics. Results Phys 2021;31:105028.
[17] Gatyeni SP, Chukwu CW, Chirove Faraimunashe, Nyabadza F, et al. Application of optimal control to the dynamics of covid-19 disease in South Africa. medRxiv; 2021, 2020-08.
[18] Mushanyu Josiah, Chukwu Williams, Nyabadza Farai, Muchatibaya Gift. Modelling the potential role of super spreaders on covid-19 transmission dynamics. Int J Math Model Numer Optim 2022;12(2):191–209.
[19] Chu Yu-Ming, Ali Aatif, Khan Muhammad Altaf, Islam Saeed, Ullah Saif. Dynamics of fractional order covid-19 model with a case study of saudi arabia. Results Phys 2021;21:103787.
[20] Khan Muhammad Altaf, Atangana Abdon. Modeling the dynamics of novel coronavirus (2019-ncov) with fractional derivative. Alex Eng J 2020;59(4):2379–89.
[21] El-Dessoky MM, Khan Muhammad Altaf. Modeling and analysis of an epidemic model with fractal-fractional atangana-baleanu derivative. Alex Eng J 2022;61(1):729–46.
[22] Barnard Rosanna C, Davies Nicholas G, Pearson Carl AB, Jit Mark, Edmunds W John. Projected epidemiological consequences of the omicron sars-cov-2 variant in england, december 2021 to april 2022. medRxiv; 2021.
[23] Karthikeyan Kulandhivel, Karthikeyan Panjaiyan, Baskonus Haci Mehmet, Venkatachalam Kuppusamy, Chu Yu-Ming. Almost sectorial operators on ψ-hilfer derivative fractional impulsive integro-differential equations. Math Methods Appl Sci 2021.
[24] Rashid Saima, Sultana Sobia, Karaca Yeliz, Khalid Aasma, Chu Yu-Ming. Some further extensions considering discrete proportional fractional operators. Fractals 2022;30(01):2240026.
[25] Rashid Saima, Abouelmagd Elbaz I, Sultana Sobia, Chu Yu-Ming. New developments in weighted n-fold type inequalities via discrete generalized-proportional fractional operators. Fractals 2021.
[26] He Zai-Yin, Abbes Abderrahmane, Jahanshahi Hadi, Alotaibi Naif D, Wang Ye. Fractional-order discrete-time sir epidemic model with vaccination: Chaos and complexity. Mathematics 2022;10(2):165.
[27] Jin Fang, Qian Zi-Shan, Chu Yu-Ming, Rahman Mati ur. On nonlinear evolution model for drinking behavior under caputo-fabrizio derivative. J Appl Anal Comput 2022.
[28] Gu Yu, Khan Muhammad Altaf, Hamed YS, Felemban Bassem F. A comprehensive mathematical model for sars-cov-2 in caputo derivative. Fractal Fract 2021;5(4):271.
[29] Zha Tie-Hong, Castillo Oscar, Jahanshahi Hadi, Yusuf Abdullahi, Alassafi Madini O, Alsaadi Fawaz E, Chu Yu-Ming. A fuzzy-based strategy to suppress the novel coronavirus (2019-ncov) massive outbreak. Appl Comput Math 2021;160–76.
[30] Khan Muhammad Altaf, Ullah Saif, Farhan Muhammad. The dynamics of zika virus with caputo fractional derivative. AIMS Math 2019;4(1):134–46.
[31] Awais Muhammad, Alshammari Fehaid Salem, Ullah Saif, Khan Muhammad Altaf, Islam Saeed. Modeling and simulation of the novel coronavirus in caputo derivative. Results Phys 2020;19:103588.
[32] Iqbal Md Ashik, Wang Ye, Miah Md Mamun, Osman Mohamed S. Study on date–jimbo–kashiwara–miwa equation with conformable derivative dependent on time parameter to find the exact dynamic wave solutions. Fractal Fract 2021;6(1):4.
[33] Wang Fuzhang, Khan Muhammad Nawaz, Ahmad Imtiaz, Ahmad Hijaz, Abu-Zinadah Hanaa, Chu Yu-Ming. Numerical solution of traveling waves in chemical kinetics: time-fractional fishers equations. Fractals 2022;2240051.
[34] Nazeer Mubbashar, Hussain Farooq, Khan M Ijaz, El-Zahar Essam Roshdy, Chu Yu-Ming, Malik MY, et al. Theoretical study of mhd electro-osmotically flow of third-grade fluid in micro channel. Appl Math Comput 2022;420:126868.
[35] Zhao Tie-Hong, Khan M Ijaz, Chu Yu-Ming. Artificial neural networking (ann) analysis for heat and entropy generation in flow of non-newtonian fluid between two rotating disks. Math Methods Appl Sci 2021.

[36] Khan MA, Ali K, Bonyah E, Okosun KO, Islam S, Khan A. Mathematical modeling and stability analysis of pine wilt disease with optimal control. Sci Rep 2017;7(1):1–19.
[37] Alderremy AA, Gómez-Aguilar JF, Aly Shaban, Saad Khaled M. A fuzzy fractional model of coronavirus (covid-19) and its study with legendre spectral method. Results Phys 2021;21:103773.
[38] Alqhtani Manal, Saad Khaled M. Fractal–fractional michaelis–menten enzymatic reaction model via different kernels. Fractal Fract 2021;6(1):13.
[39] Alqhtani Manal, Saad Khaled M. Numerical solutions of space-fractional diffusion equations via the exponential decay kernel. AIMS Math 2022;7(4):6535–49.
[40] Asghar Atifa, Khan Muhammad Altaf, Iskakova Kulpash, Al-Duais Fuad S, Ahmad Irshad. Mathematical modeling and analysis of the sars-cov-2 disease with reinfection. Comput Biol Chem 2022;107678.
[41] Gumel Abba B, Iboi Enahoro A, Ngonghala Calistus N, Elbasha Elamin H. A primer on using mathematics to understand covid-19 dynamics: Modeling, analysis and simulations. Infect Dis Model 2021;6:148–68.
[42] Shen Zhong-Hua, Chu Yu-Ming, Khan Muhammad Altaf, Muhammad Shabbir, Al-Hartomy Omar A, Higazy M. Mathematical modeling and optimal control of the covid-19 dynamics. Results Phys 2021;31:105028.
[43] Driessche Pauline Van den, Watmough James. Reproduction numbers and sub-threshold endemic equilibria for compartmental models of disease transmission. Math Biosci 2002;180(1–2):29–48.
[44] Salle Joseph La, Lefschetz Solomon. Stability by Liapunov's direct method with applications by joseph l salle and solomon lefschetz. Elsevier; 2012.
[45] Toufik Mekkaoui, Atangana Abdon. New numerical approximation of fractional derivative with non-local and non-singular kernel: application to chaotic models. Eur Phys J Plus 2017;132(10):1–16.
[46] Atangana Abdon, Araz Seda İğret. New concept in calculus: Piecewise differential and integral operators. Chaos Solitons Fractals 2021;145:110638.
[47] Atangana Abdon, Araz Seda İğret. Modeling third waves of covid-19 spread with piecewise differential and integral operators. Turkey, spain and czechia: medRxiv; 2021.
[48] Khan Muhammad Altaf, Atangana Abdon. Mathematical modeling and analysis of covid-19: A study of new variant omicron. Physica A 2022;127452.
[49] World / countries / south africa, daily new cases in south africa https://www.worldometers.info/coronavirus/country/south-africa/.